Infrared measurements of fluid temperature in a polymeric Pulsating Heat Pipe

L Pagliarini[1,*], F Clemens[2], F Bozzoli[1], L Cattani[1], N Miche[2], M Bernagozzi[2], M Marengo [2,3], A A Alqahtani[4], V Bertola[4]

[1]Department of Engineering and Architecture, University of Parma, Parco Area delle Scienze 181/A, I-43124 Parma, Italy
[2]Advanced Engineering Centre, School of Architecture, Technology and Engineering, University of Brighton, Lewes Road BN24GJ, United Kingdom
[3]Department of Civil Engineering and Architecture, University of Pavia, Via Ferrata 3, Pavia, Italy
[4]Laboratory of Technical Physics, University of Liverpool, Brownlow Hill, Liverpool L69 3GH, United Kingdom

* Corresponding author: luca.pagliarini@unipr.it

Abstract. Pulsating heat pipes are two-phase passive heat transfer devices partially filled with a working fluid in saturation conditions. During operation, supplying heat to one end of the system (named evaporator) results in a local increase in temperature and pressure, which drives the fluid through a transport section (named adiabatic section) towards the cooled, opposite end (named condenser) for effective heat dissipation. The local thermo-fluid dynamic state of the working fluid is sometimes assessed by means of non-intrusive techniques, such as infrared thermography. In this case, the radiative properties of the systems in the infrared spectrum must be known a priori. Nevertheless, since pulsating heat pipes may be manufactured with different materials, wall thicknesses and channel geometries, the radiative properties of the walls and the confined flow are not always known or assessable by means of the available literature. Hence, the work proposes to design a straightforward calibration procedure for quantitative infrared fluid temperature measurements in a polymeric pulsating heat pipe charged with FC-72 and having unknown radiative properties. The emissivity and transmissivity of the walls and confined fluid are estimated with good accuracy. The results will allow repeatable and reliable fluid temperature measurements in future experimentations on the mentioned device.

1. Introduction

Effective and reliable heat transfer devices are required for a substantial reduction in energy consumption for electronics cooling. Two-phase systems are widely used in thermal management applications [1]. However, standard active two-phase devices, which rely on the employment of auxiliary equipment, are not efficient from an energetic standpoint [2]. On the contrary, passive devices are characterized by spontaneous heat dissipation, thus representing an attractive solution to the energy issue. In particular, Pulsating Heat Pipes (PHPs) are achieving resounding interest within the academic and industrial communities due to their high flexibility, high heat transfer efficiency and low manufacturing cost, when compared to other passive systems, e.g., Heat Pipes (HPs). In their most common and simplest layout, PHPs are constituted by a capillary evacuated tube bent in many turns and filled with a working fluid in saturation conditions, thus presenting an alternation of liquid slugs and vapor plugs. Three main sections are often identified: the evaporator zone, where heat is supplied, the condenser zone, where heat is dissipated, and the adiabatic section, where the device does not thermally interact with the external environment [3]. Heat dissipation is guaranteed by self-sustained oscillations of the working fluid, induced by temperature differences between the evaporator and the condenser. Such thermal instabilities result in pressure differences acting as pumping forces for a spontaneous fluid motion [4]. Nevertheless, the very complex non-equilibrium thermodynamics underlying the PHPs physics undermines a clear and full understanding of their working behaviour. In addition, the experimental approaches usually adopted for the study of PHPs lack of completeness and generality. This is due to the fact that the PHPs operation is generally assessed from global characterizations, based on measurements over time of both evaporator and condenser temperatures [5]. A local evaluation of the fluid thermodynamics state is instead rarely achieved ([6–8]) due to difficulties linked to sensors placement inside the fluid stream without increasing the set-ups complexity or perturbing the system [9]. On the other hand, devices having transparent inserts or windows might be investigated in terms of working fluid temperature by means of non-intrusive techniques, such as InfraRed (IR) thermography. Mameli et al. [10] carried out IR investigations on a sapphire insert (transmissivity provided by the manufacturer) in a multi-turn PHP having inner diameter equal to 3 mm. The device was filled with FC-72 (50% vol.) and tested under different gravity conditions. At both ends of the transparent channel, micro-thermocouples were inserted in the fluid stream to directly monitor the fluid temperature during operation. Being FC-72 (liquid phase) partially transparent to IR radiations, as suggested in [11], its temperature could be only assessed when it completely filled the tube. In fact, by comparing the fluid temperature signals recorded through micro-thermocouples and the ones recorded by the IR camera, an agreement between the two sets of data was present only when liquid passed through the section investigated by thermography. Due to the excellent sensitivity of the adopted IR camera, temperature gradients along liquid slugs could be also assessed with good accuracy, reflecting the local effects of both the evaporator and condenser sections on the fluid flow. Mangini et al. [12] performed IR acquisitions on the fluid flow through transparent inserts made of sapphire (thickness: 1 mm, inner diameter: 2 mm) in a multi-turn PHP partially charged with ethanol. Here, the transmissivity of the sapphire wall was provided by the manufacturer equal to 0.9. However, the fluid emissivity at different temperatures was unknown, preventing quantitative fluid temperature measurements. Hence, liquid ethanol was circulated at prescribed temperatures through a sapphire channel (same dimensions of the one mounted on the experimental set-up). The transparent branch was framed by an IR camera, and the outputted signals were compared with the ones obtained from the IR observation of a black body (emissivity = 0.997) at same temperatures. The two sets of IR signals were in good agreement, suggesting that ethanol (liquid phase) was perfectly opaque to infrared radiations for the considered thickness of 2 mm in between 15°C and 35°C. The vapour phase was instead found to be fully transparent. The calibration loop shown in [12] was similar to the one adopted in [11]. However, the estimation of IR properties by using a dedicated calibration loop is not always feasible due to possible difficulties in the manufacturing process or presence of complex layouts (e.g., micro or flexible geometries).

The present work proposes to design a straightforward technique to estimate radiative properties of a polymeric PHP partially filled with FC-72 for the sake of future experimentations, without substantial modifications on the layout or dedicated experimental apparatuses. The main challenge is represented by the fact that both the device walls and the confined fluid are partially transparent in the IR spectrum. Hence, the wall, fluid and background temperatures must be carefully monitored during calibration. The charged device is kept at prescribed temperature inside a thermal chamber. The background temperature is controlled by means of a thermostatic loop. IR acquisitions are carried out during steady state. By adopting a radiation model that considers emissions and transmissions of all the radiative elements in the system, emissivity and transmissivity of both working fluid and PHP walls (partially transparent in the IR spectrum) are estimated through a minimization approach. The proposed technique will be used to achieve quantitative fluid temperature measurements by means of thermography on the investigated device. The procedure could be replicated for IR analyses of other partially transparent devices, whose geometry and material do not allow feasible manufacturing of a calibration loop.

2. Experimental set-up

The studied PHP (6 turns in the evaporator section, 5 turns in the condenser section) is made of polypropylene, with 3 x 0.7 mm rectangular channels (Figure 1a). In particular, polypropylene is chosen for fabrication to guarantee high degree of foldability and consequent high flexibility for different kinds of application [13], as shown in Figure 1b.

a) b)

Figure 1. Studied device (a) and its potential foldability (b).

The serpentine channel is cut-out in a black sheet (0.7 mm thickness) using a commercial laser cutter (HPC® Laser LS1290 Pro). Then, the channel is sandwiched between two transparent sheets (0.4 mm thickness each), which were tightly bonded to the black sheet by selective transmission laser welding using a nanosecond pulsed fiber (SPI® Lasers G4 HS-L 20 W). A micro-metering valve, mounted on an aluminum clamp screwed on the PHP, is used for the filling/vacuuming procedure. For further details on the manufacturing processes, see [14].

A calibrated IR camera (TELOPS® FAST-IR M100K, pixel resolution: 1280x1024, spectral bandwidth: 3 - 4.9 μm) is used to perform acquisitions on the device. Before the tests, the PHP was filled with pure FC-72 (FR = 50% vol.), previously degassed by means of iteratively warming/cooling under vacuum conditions.

For successful fluid temperature measurements by means of thermography, the following radiative properties of the system needed to be estimated since practically unknown for the given application (i.e., for the PHP walls and fluid thicknesses):

- Emissivity and transmissivity of the polypropylene walls;
- Emissivity and transmissivity of FC-72 (liquid phase), when confined inside the device channels.

Specifically, to achieve a good characterization of the PHP radiative behaviour in the IR spectrum, the effects of the background and of the emissive elements constituting the PHP, such as the polypropylene walls and the working fluid, should be separately taken into consideration. Hence, the background emissivity and temperature must be known, together with the temperature of the emissive elements. To this aim, a copper plate, which surface was coated with a high-emissivity paint (ε = 0.92), and which temperature was controlled by a thermal bath, was placed behind the device (Figure 2a).

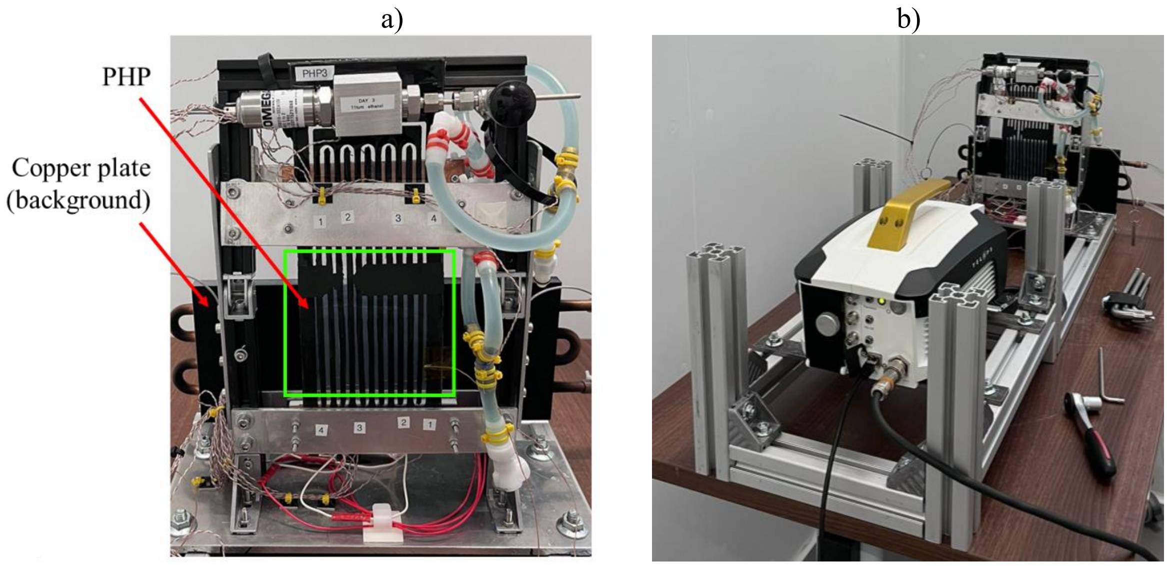

Figure 2. Experimental apparatus, with reference to the area framed by the camera (green box) and background position (a); test bench, located inside the thermostatic chamber (b).

The set-up was therefore introduced inside a thermostatic chamber (accuracy = ± 1°C), as shown in Figure 2a; this guaranteed that, at steady-state conditions, the temperature of all the emissive elements but the background was equal to the set-point temperature of the chamber.

The PHP was tested without triggering its activation by means of any heat load at the evaporator, and two IR pictures were taken when thermal equilibrium with the chamber environment was reached. Specifically, the portion framed by the IR camera during acquisitions is shown in Figure 2a (green box). In Table 1, the pairs of background and ambient temperature set-points imposed over a total of 7 different tests are listed.

Table 1. Temperature set-points imposed during the tests.

Test number	Background temperature set-point [°C]	Ambient temperature set-point [°C]
1	55	20
2	19	25
3	21	25
4	18	30
5	22	30
6	19	35
7	22	35

Two T-type thermocouples were placed on the background surface and on the PHP wall, respectively, to assess the accuracy of the given set-point temperatures.

3. Methods

3.1. Radiation model

The adopted radiation model is described by the energy flow diagram of Figure 4. Specifically, the IR radiation acquired by the IR camera sensors Q_{IR} is a combination of radiations emitted by the background Q_{BG}, the PHP walls Q_w' and Q_w'', and the working fluid Q_f, net of losses through the device elements (walls and fluid) due to their non-unitary transmissivity in the IR spectrum.

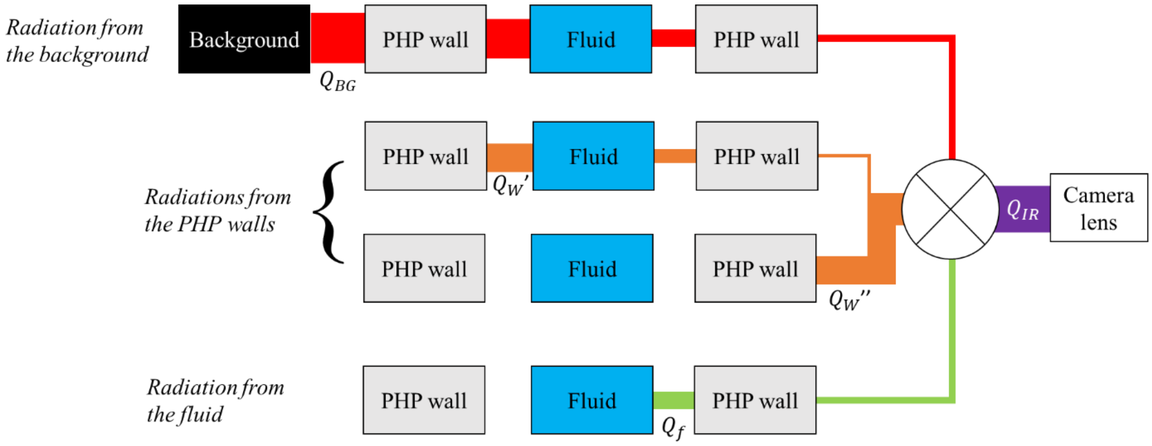

Figure 3: Radiation model.

Such a radiation model can be formalized by Equation (1), where the subscript *net* stands for net IR radiation reaching the camera lens.

$$Q_{IR} = Q_{BG,net} + (Q_{w,net}{}' + Q_w{}'') + Q_{f,net} \qquad (1)$$

By furtherly considering the temperature and radiative properties of each emissive element, Equation (1) reads as:

$$Q_{IR} = \sigma\varepsilon_{BG}\tau_{PHP}\tau_f T_{BG}^4 + \sigma\left[\left(1+\tau_{PHP}^{1/2}\right)\tau_f\right]\varepsilon_w T_w^4 + \sigma\varepsilon_f\tau_{PHP}^{1/2}T_f^4 \qquad (2)$$

where σ is the Stefan-Boltzmann constant, ε_{BG} is the emissivity of the background, τ_{PHP} is the transmissivity of both PHP walls ($\tau_{PHP}^{1/2}$ for the single wall), T_{BG} is the background temperature, τ_f is the transmissivity of the fluid, ε_w is the emissivity of the single PHP wall, T_w is the wall temperature, and ε_f is the fluid emissivity.

3.2. Radiative properties evaluation

The radiative properties of all the emissive elements were evaluated by considering areas containing both vapour and liquid phases. To discern the two phases, a coefficient *c* was introduced in (1):

$$Q_{IR} = \sigma\varepsilon_{BG}\tau_{PHP}\tau_f^c T_{BG}^4 + \sigma\left[\left(1+\tau_{PHP}^{1/2}\right)\tau_f^c\right]\varepsilon_w T_w^4 + c\sigma\varepsilon_f\tau_{PHP}^{1/2}T_f^4 \qquad (3)$$

Such a coefficient was set to 0 when the vapour phase was observed, and to 1 when the liquid phase was instead investigated. Hence, τ_{PHP}, ε_w, τ_f and ε_f (liquid phase) were assessed through the resolution of the following minimization problem:

$$\min_{\tau_w,\varepsilon_w,\tau_f,\varepsilon_f\in R^+}\left[Q_{IR} - \sigma\varepsilon_{BG}\tau_{PHP}\tau_f^c T_{BG}^4 - \sigma\left[\left(1+\tau_{PHP}^{1/2}\right)\tau_f^c\right]\varepsilon_w T_w^4 - c\sigma\varepsilon_f\tau_{PHP}^{1/2}T_f^4\right] \quad ; \quad \tau_w,\varepsilon_w,\tau_f,\varepsilon_f < 1 \qquad (4)$$

4. Results

As mentioned in Section 3.2, IR acquisitions were processed by discerning liquid phase from vapour phase. It has to be pointed out that, since the device was not fully filled with FC-72, the liquid phase tended to stratify due to gravity and vibrations at the bottom of the channels, as noticeable from the IR sample of Figure 4.

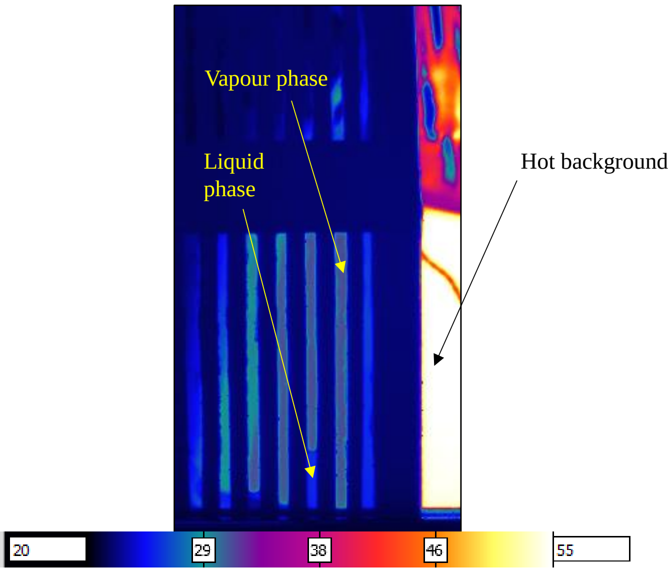

Figure 4. IR acquisition sample; system at 20°C, hot background at 55°C.

Q_{IR} referred to all pixels within each framed PHP channel was used as input for Equation (4). Specifically, the data collected during every test condition listed in Table 1 were considered at the same time in the minimization problem resolution. All the estimated radiative properties are shown in Figure 5, along with the 95% confidence intervals. In particular, the intervals have been estimated through a nonlinear regression, adopting the jacobian and residual outputs given by the combination of MATLAB® (v. R2022b) functions *nlinfit* and *nlparci*. To the Authors' knowledge, the literature does not provide radiative properties for the specific thicknesses and temperatures adopted in the present investigation, especially in the wavelength range of the adopted IR camera. Anyway, the estimated values are in good agreement with [15] for what concerns the FC-72 emissivity, and with [16] regarding the polypropylene wall transmissivity, confirming the goodness of the approach.

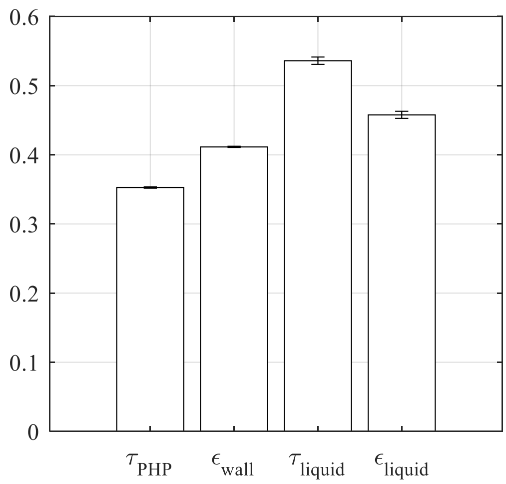

Figure 5: Evaluated radiative thermal properties of the PHP elements.

The estimation of the radiative properties of the system will be used, in future studies, for the fluid temperature evaluation during its operation in microgravity and standard-gravity conditions. It has to be stressed that, since during experimentations the wall temperature is not usually monitored in every part of the device, Equation (2) cannot be directly used to quantify T_f in the overall system. However, a simple yet effective assumption may be adopted, such as considering the wall temperature equal to the average between the fluid temperature and the environmental temperature T_{env}, $T_w = (T_{env} + T_f)/2$. Such assumption might be correct when focusing on the PHP adiabatic section (area of interest for the present investigation), according to [17], especially when the adiabatic zone is not thermally insulated for visualization purposes. T_f is therefore estimated by finding the real, positive root of the following fourth-order polynomial, coming from a rearrangement of Equation (2):

$$\left[\tau_f \varepsilon_w \left(1 + \tau_{PHP}^{1/2}\right) + \frac{\varepsilon_f \tau_{PHP}^{1/2}}{16}\right] T_f^4 + \left[\frac{T_{env} \tau_f \varepsilon_w}{4}\left(1 + \tau_{PHP}^{1/2}\right)\right] T_f^3 + \left[\frac{3}{8} T_{env}^2 \tau_f \varepsilon_w \left(1 + \tau_{PHP}^{1/2}\right)\right] T_f^2 + \left[\frac{T_{env}^3 \tau_f \varepsilon_w}{4}\left(1 + \tau_{PHP}^{1/2}\right)\right] T_f + \frac{T_{env}^4 \tau_f \varepsilon_w}{16}\left(1 + \tau_{PHP}^{1/2}\right) + \varepsilon_{BG} \tau_{PHP} \tau_f T_{BG}^4 - Q_{IR} = 0 \tag{5}$$

5. Conclusions

A polymeric pulsating heat pipe, partially filled with FC-72, was studied by means of thermography to estimate the radiative properties of the device walls and confined fluid (liquid phase). In fact, the literature does not generally provide references for the radiative properties of materials and fluids which are suitable for any investigated geometry and application. Hence, a calibration procedure, relying on a dedicated radiation model for the system, was proposed without fabricating complex calibration peripherals, such as calibration loops. To control the wall, fluid and background temperatures, a copper plate at prescribed temperature was placed behind the device, and the set-up was inserted into a thermostatic chamber. Different set-point temperatures were given to the chamber and the background, and infrared samples were taken once the system reached the steady state. By solving a minimization problem, the transmissivity and emissivity of the device walls and working fluid were found equal to 0.36, 0.42, 0.53 and 0.46, respectively. The estimated radiative properties will be adopted, in future experimentations, for fluid temperature measurements by means of thermography in the operating device.

6. References

[1] Mousa M H, Yang C M, Nawaz K, Miljkovic N, Review of heat transfer enhancement techniques in two-phase flows for highly efficient and sustainable cooling, Renewable and Sustainable Energy Reviews. 155 (2022) 111896. https://doi.org/https://doi.org/10.1016/j.rser.2021.111896.

[2] Sohel Murshed S M, Nieto de Castro C A, A critical review of traditional and emerging techniques and fluids for electronics cooling, Renewable and Sustainable Energy Reviews. 78 (2017) 821–833. https://doi.org/10.1016/J.RSER.2017.04.112.

[3] Marengo M, Nikolayev V S, Pulsating Heat Pipes: Experimental Analysis, Design and Applications, (2018) 1–62. https://doi.org/10.1142/9789813234406_0001.

[4] Spinato G, Borhani N, Thome J R, Understanding the self-sustained oscillating two-phase flow motion in a closed loop pulsating heat pipe, Energy. 90 (2015) 889–899. https://doi.org/https://doi.org/10.1016/j.energy.2015.07.119.

[5] Alhuyi Nazari M, Ahmadi M H, Ghasempour R, M.B. Shafii, Mahian O, Kalogirou S, Wongwises S, A review on pulsating heat pipes: From solar to cryogenic applications, Appl Energy. 222 (2018) 475–484. https://doi.org/https://doi.org/10.1016/j.apenergy.2018.04.020.

[6] Jun S, Kim S J, Experimental investigation on the thermodynamic state of vapor plugs in pulsating heat pipes, Int J Heat Mass Transf. 134 (2019) 321–328. https://doi.org/https://doi.org/10.1016/j.ijheatmasstransfer.2019.01.053.

[7] Sun Q, Qu J, Li X, Yuan J, Experimental investigation of thermo-hydrodynamic behavior in a closed loop oscillating heat pipe, Exp Therm Fluid Sci. 82 (2017) 450–458. https://doi.org/https://doi.org/10.1016/j.expthermflusci.2016.11.040.

[8] Mameli M, Marengo M, Khandekar S, Local heat transfer measurement and thermo-fluid characterization of a pulsating heat pipe, International Journal of Thermal Sciences. 75 (2014) 140–152. https://doi.org/10.1016/j.ijthermalsci.2013.07.025.
[9] Pagliarini L, Cattani L, Mameli M, Filippeschi S, Bozzoli F, Heat transfer delay method for the fluid velocity evaluation in a multi-turn pulsating heat pipe, International Journal of Thermofluids. 17 (2023) 100278. https://doi.org/https://doi.org/10.1016/j.ijft.2022.100278.
[10] Mameli M, Pietrasanta L, Fioriti D, Di Marco P, Filippeschi S, Large Diameter Pulsating Heat Pipe for Future Experiments on the International Space Station: Ground and Microgravity Thermal Response, in Joint 19th IHPC and 13th IHPS, Pisa, Italy, June 10-14, 2018.
[11] Catarsi A, Fioriti D, Mameli M, Filippeschi S, Di Marco P, Accuracy Analysis of Direct Infrared Temperature Measurements of Two-Phase Confined Flows, (2018) 8943–8953. https://doi.org/10.1615/ihtc16.tpm.024202.
[12] Mangini S, Marengo M, Araneo L, Mameli M, Fioriti D, Filippeschi S, Infrared analysis of the two phase flow in a single closed loop pulsating heat pipe, Exp Therm Fluid Sci. 97 (2018) 304–312. https://doi.org/https://doi.org/10.1016/j.expthermflusci.2018.04.018.
[13] Article R, Plane T G, Chamber V, A Review of Heat Pipe technology for Foldable Electronic Devices, (2019).
[14] Der O, Alqahtani A A, Marengo M, Bertola V, Characterization of polypropylene pulsating heat stripes: Effects of orientation, heat transfer fluid, and loop geometry, Appl Therm Eng. 184 (2021) 116304. https://doi.org/https://doi.org/10.1016/j.applthermaleng.2020.116304.
[15] Brutin D, Sobac B, Rigollet F, Le Niliot C, Infrared visualization of thermal motion inside a sessile drop deposited onto a heated surface, Exp Therm Fluid Sci. 35 (2011) 521–530. https://doi.org/https://doi.org/10.1016/j.expthermflusci.2010.12.004.
[16] Tsilingiris P T, Comparative evaluation of the infrared transmission of polymer films, Energy Convers Manag. 44 (2003) 2839–2856. https://doi.org/https://doi.org/10.1016/S0196-8904(03)00066-9.
[17] Mameli M, Catarsi A, Mangini D, Pietrasanta L, Michè N, Marengo M, Di Marco P, Filippeschi S, Start-up in microgravity and local thermodynamic states of a hybrid loop thermosyphon/pulsating heat pipe, Appl Therm Eng. 158 (2019) 113771. https://doi.org/10.1016/j.applthermaleng.2019.113771.

Acknowledgments
The Authors would like to acknowledge the European Space Agency (ESA) support through the grant 4000128640/19/NL/PG/pt, ESA MAP project TOPDESS.